quite surprising that misreading of the base sequences during the processes of transcription and translation is quite rare in spite of the apparent arbitrariness of the hydrogen bonded site. Steric hindrance at the decoding site should be severe. On the other hand, recent x-ray analyses on tRNA show the existence of extra base pairs which differ from usual A-U and A-T pairs.[23,24] Ability of the C-2 carbonyl group to form hydrogen bonds may be important in building up a three-dimensional structure of tRNA. It is known that in place of thymine, 5-bromouracil can easily be incorporated into DNA at the duplication process and induces mutation.[25] The present experiments show that in base pairing 5-bromouracil uses the C-2 carbonyl group as a proton acceptor much more frequently than thymine. This presumably means that 5-bromouracil is more likely to give rise to mispairs like G-BrU, where the C-2 carbonyl group is used. Thus the ability to form a hydrogen-bonded complex using the C-2 carbonyl group may be related to biological processes in several cases.[26]

References and Notes

(1) R. M. Hamlin Jr., R. C. Lord, and A. Rich, *Science*, **148**, 1734 (1965).
(2) E. Kuchler and J. Derkosch, *Z. Naturforsch. B*, **21**, 209 (1966).
(3) Y. Kyogoku, R. C. Lord, and A. Rich, *Science*, **154**, 518 (1966).
(4) J. Pitha, R. N. Jones, and P. Pithova, *Can. J. Chem.*, **44**, 1045 (1966).
(5) Y. Kyogoku, R. C. Lord, and A. Rich, *J. Am. Chem. Soc.*, **89**, 496 (1967).
(6) Y. Kyogoku, R. C. Lord, and A. Rich, *Proc. Natl. Acad. Sci. U.S.A.*, **57**, 250 (1967).
(7) J. H. Miller and H. M. Sobell, *J. Mol. Biol.*, **23**, 345 (1967).
(8) Y. Kyogoku, R. C. Lord, and A. Rich, *Biochim. Biophys. Acta*, **179**, 10 (1969).
(9) R. R. Shoup, H. T. Miles, and E. D. Becker, *Biochim. Biophys. Acta*, **179**, 10 (1966).
(10) L. Katz and S. Penman, *J. Mol. Biol.*, **15**, 220 (1966).
(11) L. Katz, *J. Mol. Biol.*, **44**, 279 (1969).
(12) L. Katz, K. Tomita, and A. Rich, *J. Mol. Biol.*, **13**, 340 (1965).
(13) W. Saeuger and D. Suck, *Nature (London)*, **227**, 1046 (1970).
(14) R. M. Thomas, "Introduction to Numerical Methods and FORTRAN Programming", Wiley, New York, N.Y., 1967.
(15) O. Kikuchi, "Molecular Orbital Calculation", Kodansha, Tokyo, 1971.
(16) K. Morikawa, T. Katsura, and Y. Iitaka, unpublished.
(17) A. J. Jones, D. M. Grant, M. W. Winkley, and K. Robins, *J. Phys. Chem.*, **74**, 2684 (1970).
(18) A. D'Albis, M. P. Wickens, and W. B. Gratzer, *Biopolymers*, **14**, 1423 (1975).
(19) H. Spiesecke and W. A. Schneider, *Tetrahedron Lett.*, 468 (1961).
(20) G. C. Pimental and A. L. McClellan, "The Hydrogen Bond", W. H. Freeman, San Francisco, Calif., 1960.
(21) J. D. Watson and F. H. C. Crick, *Nature (London)*, **171**, 737 (1953).
(22) K. Hoogsteen, *Acta Crystallogr.*, **12**, 822 (1959); **16**, 907 (1963).
(23) J. D. Robertus, J. E. Lander, J. T. Finch, D. Rhodes, R. S. Brown, B. F. C. Clark, and A. Klug, *Nature (London)*, **250**, 546 (1974).
(24) S. H. Kim, F. L. Suddath, G. J. Quigley, A. MacPerson, J. L. Wang, N. C. Seeman, and A. Rich, *Science*, **185**, 435 (1974).
(25) W. Hayes, "The Genetics of Bacteria and Their Viruses", Blackwell, Oxford, 1964, p 278.
(26) The authors wish to express their thanks to Professor K. Nishimoto, Osaka Municipal University, and Dr. T. Katsura for their advice in calculation of electron charge densities.

Calculation of ^{13}C Relaxation Times and Nuclear Overhauser Enhancements in a Hydrocarbon Chain Undergoing Gauche–Trans Isomerism†

Robert E. London* and John Avitabile

Contribution from the Chemistry Division and Theoretical Division, University of California, Los Alamos Scientific Laboratory, Los Alamos, New Mexico 87545.

Received December 29, 1976

Abstract: An analytically tractable model has been developed for calculating the relaxation times of a hydrocarbon chain undergoing gauche–trans isomerization about each carbon–carbon bond and overall isotropic motion. Each internal rotation is described by two parameters, τ_t, the lifetime of a trans state, and σ, the equilibrium ratio of gauche to trans states: $\sigma = ([g^+] + [g^-])/2[t]$. Spin lattice relaxation times (T_1), spin–spin relaxation times (T_2), and nuclear Overhauser enhancements (NOE) have been calculated for a six-bond chain. As a result of the restriction introduced into the internal motion, properties associated with the slowly tumbling end of the molecule such as a reduced NOE, $T_1 \gg T_2$, and a frequency dependence of T_1 propagate far into the chain in contrast to the free internal rotation model. Analysis of data obtained for *n*-hexadecyltrimethylammonium bromide micelles and for sonicated dimyristoyl lecithin lipid vesicles indicates that restriction of internal rotation is not sufficient to explain the observed T_1 and T_2 values. For this reason, the effects of correlated motions such as kink formation and diffusion have been treated semiquantitatively and a correlation factor f introduced to reflect the degree of motional correlation. The three possible contributions to the observed T_1 gradient (cumulative effects of successive internal gauche $\rightleftarrows$ trans isomerizations as modified by an appropriate correlation factor, a gradient in the isomerization rate as described by τ_t, and a gradient in σ) are evaluated in light of available experimental data. In general, T_1 values measured in systems undergoing multiple isomerizations are found to be sensitive to the order of the system as well as to the rate of internal motion. For typical parameters, T_2 values are found to be sensitive to the degree of motional correlation and to the value of σ, but not to the isomerization rate.

I. Introduction

Nuclear magnetic resonance studies of membranes and model systems have proliferated rapidly in recent years with ^1H, ^2H, ^{13}C, ^{19}F, and ^{31}P data reported. As discussed in the recent review articles by Lee and co-workers,[1,2] the theoretical interpretations of such studies have tended to vary with the particular nucleus studied. Primarily because of the greater resolution attainable by ^{13}C NMR and the dominance of the relaxation by the ^{13}C–^1H dipolar interaction between directly bonded nuclei, the ^{13}C NMR of membrane systems has been relatively simple to interpret—a situation which is in sharp contrast with the reported ^1H NMR studies.[1,3-6] The detailed description of the ^{13}C relaxation in such lipid systems has been

† Work performed under the auspices of the U.S. Energy Research and Development Administration.

based primarily on the model originally described by Wallach[7] for multiple internal rotations, and subsequently modified by Levine and co-workers to apply to systems in which not all of the motions fall into the extreme narrowing range and to systems in which the motion of the center of mass is anisotropic.[8-10] Inherent in this model are several assumptions which must be evaluated critically in terms of their effect on the calculated relaxation times. These include:

(1) The identification of the center of mass of the molecule with a particular carbon atom in the molecule. This atom, called C_0, is then assumed to move independently (either isotropically or anisotropically) of the internal rotations occurring within the system.

(2) Each rotation is assumed to be completely independent. No correlations between the rotations about different carbon-carbon bonds are assumed to exist.

(3) Each rotation is completely free to cover a 360° range so that, for example, γ carbons occupy an eclipsed and a trans configuration with equal probability.

The free rotation model used by Levine, Metcalfe, Partington, Roberts, Lee, Birdsall, and their co-workers has several notable features. In particular, it predicts the T_1 gradient which has been observed in ^{13}C NMR studies of fatty acids in both model[12-16] and actual membrane systems.[17,18] In addition, it is consistent with the observed temperature dependence of the T_1 data. Thus, the spin-lattice relaxation is dominated by the fast internal motions with the result that T_1 should increase with increasing temperature, as it does.[11,15,17,18] Nevertheless, attempts to apply the model to various experimental results have not always met with success. For example, as noted by Lee,[1] the ^{13}C line width data obtained in either sonicated or unsonicated lipid dispersions cannot be explained by the T_2 values calculated according to Levine et al.[8] In particular, although T_1 may be much longer than T_2 for carbons near the beginning of the chain (near C_0), the calculated T_1 and T_2 values rapidly become equal as one proceeds further along the chain. This discrepancy may reflect a number of other contributions to the line width. Nevertheless, in view of the approximations made above, it is reasonable to ask whether replacing the above assumptions with more physically reasonable models would predict T_2 values more consistent with the observed line widths. In fact, as shown by the calculations given here, this turns out to be the case; as the chain conformation is weighted more heavily with trans configurations about the various carbon-carbon bonds, the ratio T_1/T_2 falls off more slowly than in the free rotation model. The effect of certain correlated motions produces a similar result and can be considered semiquantitatively.

Despite the obvious defects of the third approximation above and the possibility of obtaining numerical results for a more physically reasonable model, surprisingly little work has been done. An initial Monte Carlo calculation by Levine[19] in which the orientational autocorrelation function, but no relaxation times, were calculated indicated a surprising pairing effect so that carbons 1 and 2, 3 and 4, etc., exhibit similar autocorrelation functions and, presumably, similar relaxation times. The degree of pairing was found to be a function of the parameter $\sigma \equiv ([g^+] + [g^-])/2[t]$. This calculation was based on the statistical weight matrix given by Flory for a polymethylene chain.[20]

In this paper a slightly simplified model is considered in which the g^+g^- configuration about adjacent bonds is not completely forbidden as in the Levine-Flory treatment. Using the parameter σ defined above to represent the ratio of total gauche to trans states about a given bond, the probability of having adjacent gauche bonds is proportional to σ^2. Whether the effect of intermolecular interactions is considered to reduce σ in which case a value as small as 0.05 can be calculated,[21,22] or to correlate the internal isomerizations leading primarily to kinked conformations in which two gauche states are separated by a trans state,[23] the resulting probability of adjacent gauche states will be minimal so that the neglect of differences in the probability of occurrence of g^+g^+ and g^+g^- states should be an excellent approximation. Models based on independent gauche $\rightleftarrows$ trans isomerization have been used previously in the analysis of spin label order parameters.[24] With the above simplification of independent rotation about adjacent bonds, an analytical calculation of the correlation function and hence the T_1, T_2, and NOE values can be carried out. In the model proposed in this paper transitions of the form $g^+ \rightleftarrows g^-$ are forbidden as they are in Levine's model,[19] since such transitions go through an eclipsed intermediate state. The interconversion, therefore, between g^+ and g^- takes place via $g^+ \rightleftarrows t \rightleftarrows g^-$ transitions. If direct $g^+ \rightleftarrows g^-$ transitions are to be allowed, a simple modification of the procedure used here can be made.

II. Theory

It is generally assumed that a carbon-13 atom in a lipid chain relaxes by a dipole-dipole interaction with its directly bonded hydrogens. To calculate the relaxation times T_1 and T_2 for a given carbon, therefore, it is necessary to determine the orientational autocorrelation function of the carbon-hydrogen bond. For a lipid chain rotating isotropically about its head group, Wallach[7] has shown that the autocorrelation function of the carbon-hydrogen bond for the Nth carbon in the chain is given by the expression

$$G_N(\tau) = \sum_{\substack{a,b,c\ldots n \\ b',c'\ldots n'}} \exp -(6D_0\tau) d_{ab}(\beta) d_{ab'}(\beta) d_{bc}(\beta) d_{b'c'}(\beta) \ldots \times \ldots d_{n0}(\beta') d_{n'0}(\beta') \langle \exp i[a\gamma_1(0) - a\gamma_1(\tau)] \ldots \times \ldots \exp i[n\gamma_N(0) - n'\gamma_N(\tau)] \rangle \quad (1)$$

where D_0 is the isotropic, rotational diffusion constant for the lipid's head group; β is the polar angle between successive carbon-carbon bonds along the chain (for saturated chains this angle is just the complement of the tetrahedral angle, 109.5°); β' is the polar angle between the $(N-1)$th carbon-carbon bond and the Nth carbon-hydrogen bond; $\gamma_1, \gamma_2, \ldots, \gamma_N$ are the respective azimuthal angles between successive bonds in the chain; and $d_{i0}(\beta)$ is the reduced Wigner rotation matrix.[25] All summations run from -2 to $+2$. The angular brackets represent an ensemble average, and τ is the time variable.

In order to evaluate $G_N(\tau)$, one must hypothesize an algorithm for calculating the ensemble average in eq 1. Specifically, this average depends on the various internal configurations and motions of the individual carbon-carbon bonds in the lipid chain. It is postulated here that each carbon-carbon bond can exist in and jump between only three states: trans (t), gauche plus (g^+), and gauche minus (g^-). Since it is sterically unfavorable, direct jumps between g^+ and g^- states are disallowed.

As noted in the Introduction, tandem g^+g^- states are not disallowed in the model but are increasingly improbable as g^+ and g^- individually become less probable. It should also be noted that disallowing adjacent g^+-g^- states is at best only a first-order approximation. It does not eliminate all excluded volume problems from the model; nor is it the only possible physical mechanism for producing correlated motions, since intermolecular forces probably play a dominant role in correlating the bond motions of a single chain.

With the hypothesis that carbon-carbon bonds move independently of each other the ensemble average in eq 1 may be simplified:

$$G_N(\tau) = \sum_{\substack{a,b,c,\ldots n \\ b',c',\ldots n'}} \exp -(6D_0t)d_{ab}(\beta)d_{ab'}(\beta)\ldots d_{n0}(\beta')d_{n'0}(\beta') \times \langle \exp ia[\gamma_1(0) - \gamma_1(\tau)]\rangle \ldots \times \langle \exp i[n\gamma_N(0) - n'\gamma_N(\tau)]\rangle \quad (2)$$

Since each bond is assumed to exist in only one of three states, t, g^+, or g^-, it follows that each azimuthal angle γ can only range over three possible values, which are arbitrarily postulated to be 0, $2\pi/3$, and $-2\pi/3$, respectively. Calculating the ensemble average over these three states requires that the probabilities of being in each one of them be known as functions of time. A simple set of decay equations may be used to evaluate these probabilities:

$$\frac{d[t]}{d\tau} = -\frac{[t]}{\tau_t} + \frac{1}{\tau_g}\{[g^+] + [g^-]\}$$
$$\frac{d[g^+]}{d\tau} = \frac{[t]}{2\tau_t} - \frac{[g^+]}{\tau_g}$$
$$\frac{d[g^-]}{d\tau} = \frac{[t]}{2\tau_t} - \frac{[g^-]}{\tau_g} \quad (3)$$

where τ_t and τ_g are the respective lifetimes of the trans and gauche configurations; the bracketed quantities represent the probabilities of the given states, and it is assumed that gauche states can make transitions only to trans states. In the steady state, eq 3 can be reduced to a single relationship

$$\frac{2[t]}{[g^+] + [g^-]} = \frac{2\tau_t}{\tau_g} \equiv \frac{1}{\sigma} \quad (4)$$

where σ is defined to be the relative probability of being in a gauche vs. trans state divided by 2. Normalizing the total configurational probability to 1,

$$[t] + [g^+] + [g^-] = 1 \quad (5)$$

and using eq 4 one can easily solve eq 3:

$$[t] = \frac{1 + A_0 \exp[-\tau(1 + 2\sigma)/\tau_g]}{(1 + 2\sigma)}$$
$$[g^+] = \frac{\sigma + B_0 \exp[-\tau(1 + 2\sigma)/\tau_g]}{(1 + 2\sigma)} + C_0 \exp[-\tau/\tau_g]$$
$$[g^-] = \frac{\sigma + B_0 \exp[-\tau(1 + 2\sigma)/\tau_g]}{(1 + 2\sigma)} - C_0 \exp[-\tau/\tau_g] \quad (6)$$

where A_0, B_0, and C_0 are arbitrary constants.

In order to evaluate the correlation functions which appear in eq 2 it is necessary that the conditional probabilities of moving from one state to another be known. These conditional probabilities may be easily calculated with the relationships in eq 6.

$$p(t,\tau|t,0) = \frac{1 + 2\sigma \exp(-\tau/\tau_s)}{1 + 2\sigma}$$
$$p(g^+,\tau|g^+,0) = p(g^-,\tau|g^-,0) = \frac{\sigma + \frac{1}{2}\exp(-\tau/\tau_s)}{1 + 2\sigma} + \frac{1}{2}\exp(-\tau/\tau_g)$$
$$p(g^+,\tau|t,0) = p(g^-,\tau|t,0) = \frac{\sigma - \sigma\exp(-\tau/\tau_s)}{1 + 2\sigma}$$
$$p(t,\tau|g^+,0) = p(t,\tau|g^-,0) = \frac{1 - \exp(-\tau/\tau_s)}{1 + 2\sigma}$$
$$p(g^-,\tau|g^+,0) = p(g^+,\tau|g^-,0) = \frac{\sigma + \frac{1}{2}\exp(-\tau/\tau_s)}{1 + 2\sigma} - \frac{1}{2}\exp(-\tau/\tau_g)$$

	2	1	0	-1	-2
2	$\frac{1}{\sigma}+\sigma-2+\frac{9}{2}e^{-\tau/\tau_s}+\frac{3}{2}(1+2\sigma)e^{-\tau/\tau_g}$	$\frac{1}{\sigma}+\sigma-2+\frac{9}{2}e^{-\tau/\tau_s}-\frac{3}{2}(1+2\sigma)e^{-\tau/\tau_g}$	$\frac{1}{\sigma}-2\sigma+1$	$\frac{1}{\sigma}+\sigma-2+\frac{9}{2}e^{-\tau/\tau_s}+\frac{3}{2}(1+2\sigma)e^{-\tau/\tau_g}$	$\frac{1}{\sigma}+\sigma-2+\frac{9}{2}e^{-\tau/\tau_s}-\frac{3}{2}(1+2\sigma)e^{-\tau/\tau_g}$
1	$\frac{1}{\sigma}+\sigma-2+\frac{9}{2}e^{-\tau/\tau_s}-\frac{3}{2}(1+2\sigma)e^{-\tau/\tau_g}$	$\frac{1}{\sigma}+\sigma-2+\frac{9}{2}e^{-\tau/\tau_s}+\frac{3}{2}(1+2\sigma)e^{-\tau/\tau_g}$	$\frac{1}{\sigma}-2\sigma+1$	$\frac{1}{\sigma}+\sigma-2+\frac{9}{2}e^{-\tau/\tau_s}-\frac{3}{2}(1+2\sigma)e^{-\tau/\tau_g}$	$\frac{1}{\sigma}+\sigma-2+\frac{9}{2}e^{-\tau/\tau_s}+\frac{3}{2}(1+2\sigma)e^{-\tau/\tau_g}$
0	$\frac{1}{\sigma}-2\sigma+1$	$\frac{1}{\sigma}-2\sigma+1$	$\frac{(2\sigma+1)^2}{\sigma}$	$\frac{1}{\sigma}-2\sigma+1$	$\frac{1}{\sigma}-2\sigma+1$
-1	$\frac{1}{\sigma}+\sigma-2+\frac{9}{2}e^{-\tau/\tau_s}+\frac{3}{2}(1+2\sigma)e^{-\tau/\tau_g}$	$\frac{1}{\sigma}+\sigma-2+\frac{9}{2}e^{-\tau/\tau_s}-\frac{3}{2}(1+2\sigma)e^{-\tau/\tau_g}$	$\frac{1}{\sigma}-2\sigma+1$	$\frac{1}{\sigma}+\sigma-2+\frac{9}{2}e^{-\tau/\tau_s}+\frac{3}{2}(1+2\sigma)e^{-\tau/\tau_g}$	$\frac{1}{\sigma}+\sigma-2+\frac{9}{2}e^{-\tau/\tau_s}-\frac{3}{2}(1+2\sigma)e^{-\tau/\tau_g}$
-2	$\frac{1}{\sigma}+\sigma-2+\frac{9}{2}e^{-\tau/\tau_s}-\frac{3}{2}(1+2\sigma)e^{-\tau/\tau_g}$	$\frac{1}{\sigma}+\sigma-2+\frac{9}{2}e^{-\tau/\tau_s}+\frac{3}{2}(1+2\sigma)e^{-\tau/\tau_g}$	$\frac{1}{\sigma}-2\sigma+1$	$\frac{1}{\sigma}+\sigma-2+\frac{9}{2}e^{-\tau/\tau_s}-\frac{3}{2}(1+2\sigma)e^{-\tau/\tau_g}$	$\frac{1}{\sigma}+\sigma-2+\frac{9}{2}e^{-\tau/\tau_s}+\frac{3}{2}(1+2\sigma)e^{-\tau/\tau_g}$

Figure 1. Elements of the A matrix defined in the text.

where

$$\frac{1}{\tau_s} = \frac{1}{\tau_t} + \frac{1}{\tau_g},$$

$p(t,\tau|t,0)$ is the probability that a bond is in the trans state at time τ given that it was in the trans state at $\tau = 0$, and the other terms are interpreted in a like manner. The probabilities that a bond is in a given state at any time can be deduced from eq 4 and 5:

$$p(t) = \frac{1}{1 + 2\sigma}, \qquad p(g^+) = p(g^-) = \frac{\sigma}{1 + 2\sigma}$$

where $p(t)$, $p(g^+)$, and $p(g-)$ are the probabilities of being in the t, g^+, and g− states, respectively.

With the above probability functions a typical ensemble average in eq 2 can be evaluated:

$$\langle \exp i[\gamma(0)m - \gamma(\tau)m']\rangle = \sum_{\gamma_0=0,2\pi/3,-2\pi/3} \sum_{\gamma=0,2\pi/3,-2\pi/3} p(\gamma_0)p(\gamma,\tau|\gamma_0,0) \times \exp i(m\gamma_0 - m'\gamma)$$
$$\langle \exp i[\gamma(0)m - \gamma(\tau)m']\rangle = \frac{\sigma}{(1 + 2\sigma)^2} A_{mm'} \quad (7)$$

where the terms of the A matrix are given in Figure 1.

Equation 2 can be rewritten using the A matrix defined in eq 7

$$G_N(\tau) = \left[\frac{\sigma}{(1 + 2\sigma)^2}\right]^N \times \sum_{abc\ldots n} \sum_{b'c'\ldots n'} \exp -(6D_0\tau)\, A_{aa}d_{ab}d_{ab'}\ldots \times \ldots A_{mm'}d_{mn}(-\beta)d_{m'n'}(-\beta)A_{nn'}d_{n0}(\beta)d_{n'0}(\beta) \times e^{-i\,2\pi/3(n-n')} \quad (8)$$

where the equation has been specifically written for a saturated hydrocarbon chain.

Figure 2 depicts some of the rotations along the chain which lead to eq 8. Figure 2a shows the reference coordinate system with its Z axis along the direction of the C_l-C_m bond. Its Y axis is out of the paper and is perpendicular to the plane which contains all the chain's carbon-carbon bonds when the chain

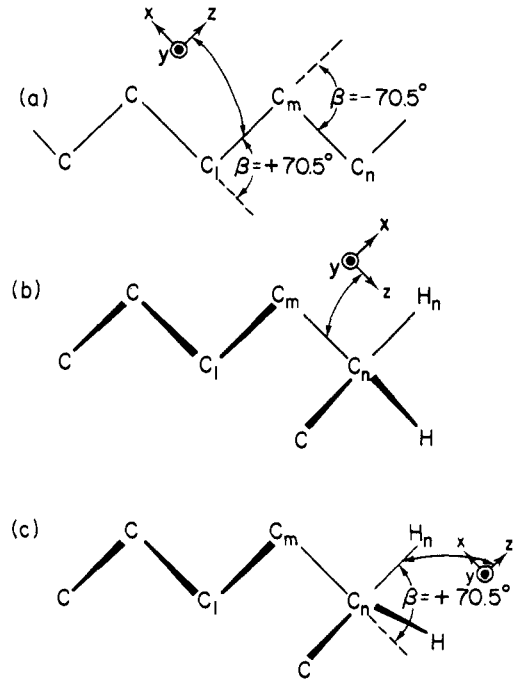

Figure 2. Orientations of the reference coordinate system relative to various positions along the hydrocarbon chain. The Y axis points out of the page in all three figures and the Z axis is always parallel to some bond in the chain. The geometry is discussed more fully in the text.

is entirely in the trans configuration. To move the reference coordinate system from its position in Figure 2a to its position in 2b, two rotations are required. First, a rotation must be performed about the Y axis through an angle of minus β ($-70.5°$). This points the Z axis of the reference coordinate system along the direction of the C_m–C_n bond and leaves the Y axis unchanged. In eq 8 this rotation is produced by using the Wigner matrices $d_{mn}(-\beta)$ and $d_{m'n'}(-\beta)$. The second rotation required to obtain 2b is through a minus 120° angle about the Z axis created by the first rotation. The Z axis direction remains unchanged while the Y axis is now perpendicular to the plane formed by the bonds C_m–C_n and C_n–H_n. The imaginary exponential in eq 8 produces this rotation. Finally, a single rotation of $+70.5°$ about the Y axis will move the reference frame from its position in Figure 2b to that in 2c. After this rotation the Z axis will lie along the direction of the C_n–H_n bond. The two matrices $d_{n0}(\beta)$ and $d_{n'0}(\beta)$ represent this final rotation in eq 8.

As a function of σ, the A matrix has the expected limiting values. When σ equals zero, and the probability that a single bond is in the trans state equals one, the quantity $\sigma/[(1 + 2\sigma)^2]A_{ab}$ equals one for all values of a and b. It then follows from eq 8 that the entire chain is in the trans state as it should be.

We have shown previously how the symmetry properties of the Wigner rotation matrices can be utilized to simplify the calculation of the correlation functions and spectral densities in systems undergoing multiple internal rotations.[26] This problem becomes even more critical at present since the direct evaluations of eq 8 or its Fourier transform are extremely laborious. In the Appendix it is shown how the symmetry properties of the A and d matrices can be used to develop an efficient computer algorithm for calculating the Fourier transform of $G_N(\tau)$ in eq 8. Once this Fourier transform is known, the standard formulas can be used for calculating T_1, T_2, and the NOE of various carbons in a model lipid chain.[8,26]

In light of the recent studies of Werbelow and Grant indicating the importance of cross correlations in determining ^{13}C relaxation behavior[27,28] we consider the orientational cross correlation function below. In deriving the autocorrelation function, eq 8, the transformation which leaves the y axis perpendicular to the C-C-H plane gives rise to the exponential term, $\exp[-i2\pi(n - n')/3]$. As a result of the summation over positive and negative indices, i.e., from -2 to $+2$, the imaginary terms drop out and a $\cos[2\pi/3(n - n')]$ factor is introduced. In order to obtain the cross correlation function we make one transformation as above and the second transformation placing the y axis perpendicular to the C-C-H′ plane, where H′ is the second methylene proton. Thus, the term $\exp[-i2\pi(n - n')/3]$ is replaced by the term $\exp[-i(n\phi_1 - n'\phi_2)]$ where $(\phi_1, \phi_2) = (\pm 2\pi/3)$. Evaluation of this term is independent of whether $\phi_1 = +$ or $-2\pi/3$. Using the coordinate system defined previously, we require $\phi_1 = -\phi_2$, so that the relevent term becomes $\exp(-i2\pi(n + n')/3)$. The sine terms vanish as above and the cosine terms give 1 for $n + n' = 3$, 6, or 9 and -0.5 otherwise. Finally, the relevent orientational cross correlation function is given by

$$G_N^{cc}(\ \ ) = \left[\frac{\sigma}{(1+2\sigma)^2}\right]^N \sum_{a,b,c,\ldots,n} \sum_{b',c',\ldots,n'} e^{-6D_0\tau} \times A_{aa}d_{ab}d_{ab'}\ldots A_{mm'}d_{mn}(-\beta)d_{m'n'}(-\beta) \times A_{nn'}d_{n0}(\beta)d_{n'0}(\beta)e^{-i(n+n')2\pi/3} \quad (9)$$

As shown by Werbelow and Grant, the inclusion of cross correlation effects leads to nonexponential decay of the spin-lattice relaxation and to altered nuclear Overhauser enhancement values. The relevent equations for determining these effects are given in ref 26-28.

III. Numerical Results and Discussion

Using the autocorrelation function defined in eq 8 values for T_1, T_2, and the NOE can be calculated based on the relations[8,29,30]

$$J(\omega) = \int_{-\infty}^{\infty} G(\tau)e^{-i\omega\tau}d\tau \quad (10)$$

$$\frac{1}{T_1} = \frac{1}{20}\frac{\gamma_H^2\gamma_C^2\hbar^2}{r_{CH}^6}[J(\omega_H - \omega_c) + 3J(\omega_c) + 6J(\omega_H + \omega_c)] \quad (11)$$

$$\frac{1}{T_2} = \frac{1}{40}\frac{\gamma_H^2\gamma_C^2\hbar^2}{r_{CH}^6} \times [J(\omega_H - \omega_c) + 3J(\omega_c) + 6J(\omega_H + \omega_c) + 4J(0) + 6J(\omega_H)] \quad (12)$$

$$\mathrm{NOE} = 1 + \frac{\gamma_H}{\gamma_C}\left[\frac{6J(\omega_H + \omega_c) - J(\omega_H - \omega_c)}{J(\omega_H - \omega_c) + 3J(\omega_c) + 6J(\omega_H + \omega_c)}\right] \quad (13)$$

Numerical results have been obtained for a six-bond chain corresponding to an isotropic rotational diffusion constant $D_0 = 10^6\ s^{-1}$ and using a trans lifetime for each internal rotation, $\tau_t = 10^{-10}$ s. The Larmor frequency for ^{13}C was chosen to be 25.2 MHz which corresponds to an applied magnetic field of 23.5 kG. The parameter σ was allowed to range from 0.001 to 1. The results of these calculations are given in Figures 3-6.

It is interesting to note the behavior of the various curves as a function of σ. The autocorrelation function contains terms proportional to $\exp(-\tau_g) = \exp(-2\sigma\tau_t)$ and $\exp(-\tau_s) = \exp[-2\sigma\tau_t/(1 + 2\sigma)]$. Thus, as σ decreases the lifetime of the gauche states decreases and the internal motion becomes more rapid. Since this motion is already in the extreme narrowing limit, it becomes even less effective in relaxing the carbons since $1/T_1 \sim \tau$ in this limit. Alternatively, as σ decreases further, the chain stiffens into the all-trans conformation. Consequently, the isotropic motion described by D_0 becomes more important. In the limit as $\sigma \to 0$, all of the carbons will relax

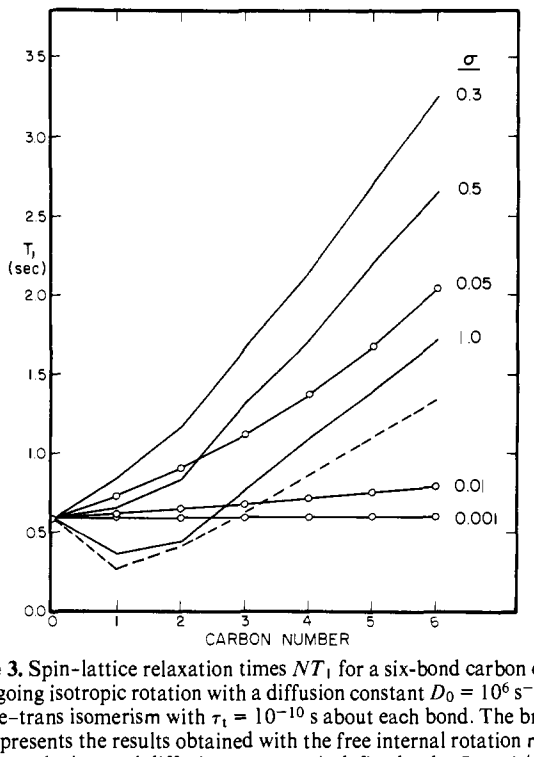

Figure 3. Spin-lattice relaxation times NT_1 for a six-bond carbon chain undergoing isotropic rotation with a diffusion constant $D_0 = 10^6\ s^{-1}$ and gauche–trans isomerism with $\tau_t = 10^{-10}$ s about each bond. The broken line represents the results obtained with the free internal rotation model where D_i, the internal diffusion constant, is defined to be $D_i = 1/6\tau_s = 1/6\tau_t(1 + 1/2\sigma)$ and $\sigma = 1.0$. The circles on the $\sigma = 0.001$, 0.05, and 0.1 curves represent calculations using the approximate matrix in which $\tau_g = \tau_s$ valid for small σ.

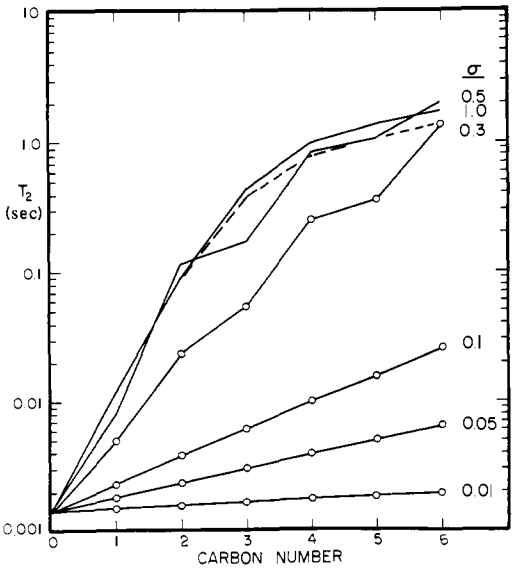

Figure 4. Spin-spin relaxation times for a six-bond carbon chain. All parameters are the same as in Figure 3. The circles represent calculations using the approximate matrix described in the text. The broken line represents a free internal rotation calculation.

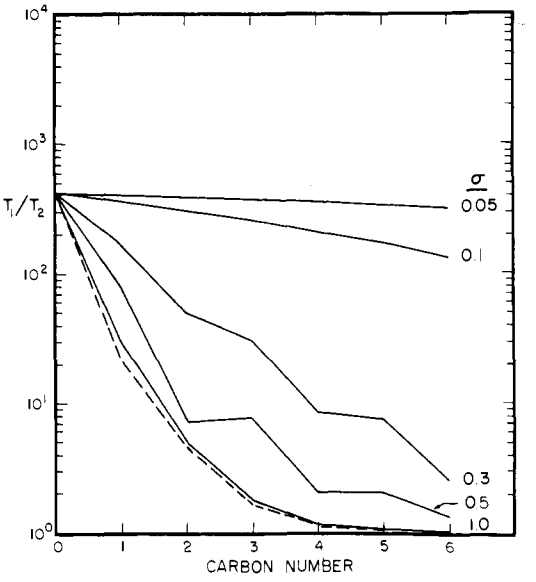

Figure 5. T_1/T_2 ratios for a six-bond methylene chain. All parameters are the same as in Figure 3. The broken line represents the free internal rotation calculation.

as if they moved isotropically with a correlation time equal to $1/6D_0$. This behavior is clearly illustrated in Figure 3. As σ decreases from 1.0 to 0.5 to 0.3, the T_1 values increase. As σ further decreases from 0.3 to 0.1 to 0.05, etc., the T_1 values decrease. The T_1 increases reflect the shorter gauche lifetimes, whereas the T_1 decreases reflect the stiffening of the chain.

A similar analysis can be applied to the free internal rotation calculation and to the gauche $\rightleftarrows$ trans isomerization calculation for $\sigma = 1.0$. The relative importance of the internal and overall motions in determining T_1 is proportional to the spectral densities corresponding to the different motions.[26] Since the isotropic motion is too slow to lead to optimal relaxation, the presence of internal motion about one bond provides a more effective spin-lattice relaxation mechanism leading to a shorter T_1. For carbons further along the chain, the cumulative effect of internal motion about each of the preceding bonds leads to an effective rate too fast for optimal relaxation so that T_1 increases with carbon number. Similarly, the effect of reducing σ is, as discussed above, to decrease τ_g and τ_s. In this case, the internal motion becomes sufficiently rapid so that T_1 does not decrease even for the first carbon. An analogous effect occurs for the free internal rotation case; in the limit in which the internal diffusion rate $D_i \rightarrow \infty$, T_1 is increased by $4/(3\cos^2\beta - 1)^2$.

An interesting feature of the calculated curves, particularly for T_2 and for T_1/T_2, is the fact that for values of σ near 0.5 they do not change smoothly as a function of the carbon number. Similarly, calculations of the orientational autocorrelation function by Levine indicated an even-odd pairing effect for similar values of σ. Thus, this result is apparently independent of the differing approximations (the possibility of consecutive g^+g^- states in the present model) between the two calculations. Interestingly, the effect appears to become less important for smaller values of σ which are applicable to the case of lipids. The physical reasons for this effect are not presently clear.

Perhaps the most significant difference between the present model and the free internal rotation model is the fact that for small values of σ the T_1/T_2 ratio changes very slowly (Figure 5). Thus, the effects of the slow isotropic motion of one end of the chain can be effectively propagated to carbons much further from C_0. This makes it possible to simulate spectra which not only have reasonable spin-lattice relaxation behavior but reasonable line widths as well. Just as the effect of the C_0 motion can have a more pronounced effect on T_2 for carbons far from C_0, the effects of the D_0 motion on the nuclear Overhauser enhancement (NOE) also extend much further along the chain (Figure 6). The $\sigma = 1.0$ case corresponds fairly closely to the case of free internal rotation which has been calculated assuming $D_i = 1/6\tau_s$.

Another significant difference between the free internal rotation model and the gauche $\rightleftarrows$ trans isomerism model developed here is the predicted frequency dependence of the spin-lattice relaxation. The T_1 values corresponding to $\nu_c =$

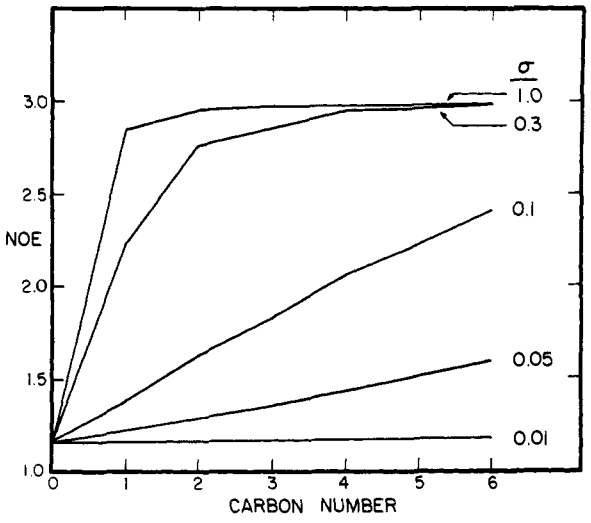

Figure 6. Nuclear Overhauser enhancement for a six-bond methylene chain. All parameters are the same as in Figure 3. The free internal rotation model gives results nearly indistinguishable from the $\sigma = 1.0$ calculation.

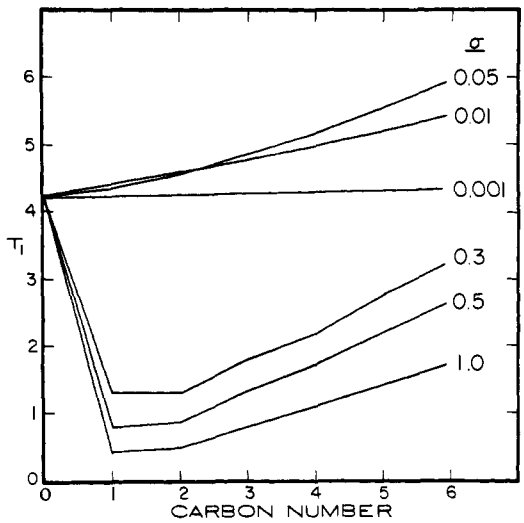

Figure 7. Spin–lattice relaxation times NT_1 for a six-bond chain calculated for $\nu_c = 67.9$ MHz ($H_0 = 63.4$ kG) for the same parameters used for the calculations given in Figure 3.

67.9 MHz and the same values of D_0 and τ_1 used in the previous calculations are given in Figure 7. For the case of $\sigma = 1.0$, essentially no frequency dependence for any carbon except C_0 is apparent, although C-1 does show a small effect. Alternatively, for smaller values of σ a pronounced frequency dependence can be observed. The most dramatic effect is observed for $\sigma \rightarrow 0$. In this limit, T_1 remains constant at the value for C_0. Since the D_0 motion is sufficiently slow, $T_1(C_0) \sim \nu^2$ so that the ratio of the T_1 values measured at the two frequencies is constant along the chain with a value of $(67.9/25.2)^2 = 7.24$ (although the ratio of the carbon frequencies is used here, all of the spectral densities will give the same ratio). A comparison of the results of Figure 3 and 7 clearly indicates this result. The frequency dependence of the T_1 values also illustrates the previous discussion regarding the behavior of T_1 as a function of σ. At the higher frequency, the slow motion corresponds to a considerably smaller spectral density and is consequently less competitive with the more rapid (extreme narrowing limit) internal motion. Consequently, the dip in the T_1 curves becomes much more pronounced and can be observed for $\sigma = 1.0$, 0.5, and 0.3 in contrast with the low-frequency calculations.

In contrast to the T_1 behavior, calculations of T_2 at the two frequencies noted above exhibit essentially no frequency dependence. This result is not surprising since the D_0 motion is sufficiently slow so that T_2 will be dominated by the zero frequency spectral density, $J(0)$ (eq 12).

Several preliminary calculations have been made to determine the effect of cross correlations on the relaxation behavior in the gauche $\rightleftarrows$ trans isomerization model. Particularly relevant is the fact that the ratio of the coefficients of the two decays becomes very large in the limit $\sigma \rightarrow 0$. Such behavior is not surprising since as $\sigma \rightarrow 0$ the motion of the lipid becomes isotropic with a diffusion coefficient of D_0. This result is of practical importance since it suggests that for real lipid systems in which σ is fairly small, cross correlations will not lead to markedly nonexponential decay. Alternatively, this result may not hold if the motion of the head group is markedly anisotropic. Further calculations of the effects of cross correlations are currently being carried out.

IV. The Effects of Correlated Rotations

Correlated rotations in hydrocarbon chains have been discussed in connection with ^{1}H NMR studies,[31-34] deuterium order parameter studies,[35-37] and, more recently, ^{13}C relaxation measurements.[38] The primary reason for postulating the existence of such correlations is that simultaneous rotations can have the effect of preserving the general linearity of the fatty acid conformation in contrast to isolated gauche orientations which introduce a large bend into the fatty acid chain. The most likely models for such correlated motion include the β coupled isomerism which can lead to "kink" formation or annihilation, as well as a δ coupled isomerism which can lead to kink diffusion[31,39] (Figure 8). It is straightforward to analyze the effects of such correlated motions semiqualitatively. If the β coupled rotations occur simultaneously and in the opposite sense, the effect on carbons further along the chain is a pure translation. Such motion will not lead to ^{13}C relaxation. If the δ coupled isomerism around a kink is completely correlated, there is no motion of carbons further along the fatty acid chain (Figure 8).

It should be emphasized that the important physical effect which is under consideration here is the simultaneity of the correlated motions. This reflects the fact that if a bond begins a $t \rightarrow g^+$ jump it will frequently not be allowed to go to completion because of the large bend which it would introduce in the fatty acid chain. Alternatively, if simultaneously a second bond β relative to the first begins to execute a $t \rightarrow g^-$ jump, the conformational changes induced by the two jumps will partially cancel out so that both jumps will be allowed to go to completion. Preliminary calculations of the relaxation effects of small, $\pm 20°$ displacements from the trans conformation suggest that such motions do not provide an effective relaxation mechanism. The lower jumping probability which results because only such correlated motions are allowed can be taken into account in the model developed in the previous section merely by using longer values of τ_1. Alternatively, inclusion of the effects of simultaneous, correlated motions requires additional considerations.

Using either the free or restricted internal rotation model, it is clear that the relaxation times obtained for the Nth carbon are functions of the diffusion coefficients $D_0, D_1, D_2, \ldots, D_N$, but not D_{N+1}, D_{N+2}, etc. This point has been emphasized by Lee, who points out that a T_1 gradient can result from a constant value of D_i.[1] The effect of correlated rotations about the C_0–C_1 bond and the C_2–C_3 bonds is therefore to eliminate the effect of diffusion described by D_1 and D_3 on the relaxation of C_N. If all the diffusion coefficients for internal rotation are identical, atom N in such a system with correlated rotations about bonds 1 and 3 will behave like atom $N - 2$ in an uncorrelated system. Therefore, a semiquantitative way to take account of such correlations is to do a calculation neglecting

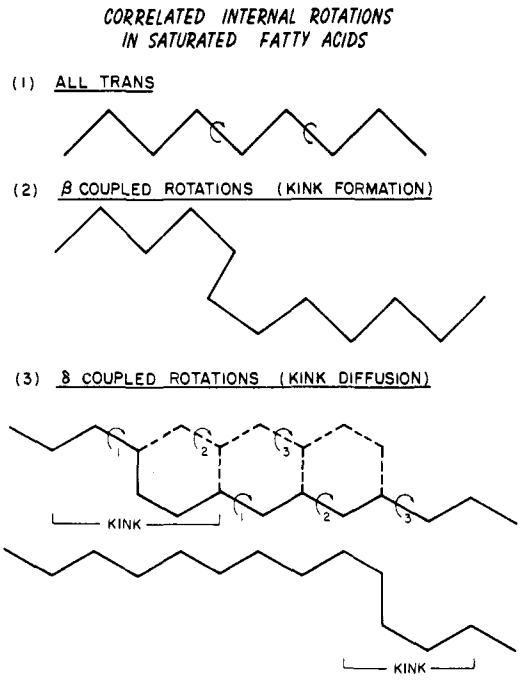

Figure 8. Possible correlated motions in a hydrocarbon chain which can reduce the T_1 and T_2 gradients as discussed in the text.

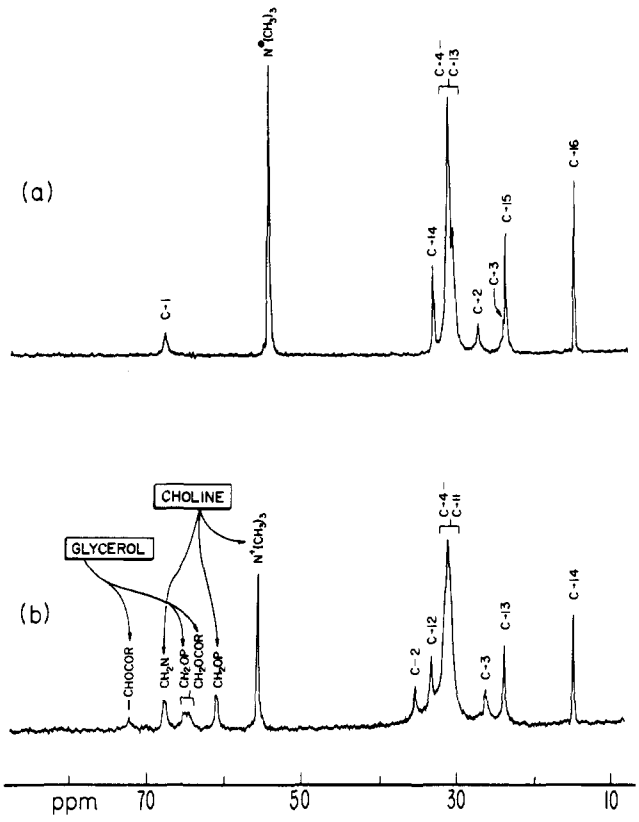

Figure 9. Proton decoupled ^{13}C NMR spectra of (a) *n*-hexadecyltrimethylammonium bromide micelles in D_2O at 42 °C and (b) sonicated L-α-dimyristoyllecithin in D_2O at 52 °C (fatty acyl carbonyl resonances not shown).

correlations and then assign to carbon N in the actual chain the relaxation times calculated for carbon fN in the (uncorrelated) model chain. The correlation parameter f varies between 0 and 1 and is a measure of how complete the correlations of the various motions are. If, for example, $f = 0.2$, it is only necessary to do an internal rotation calculation for a four-carbon chain to describe the relaxation in a 20-carbon chain for which the motion is assumed to be correlated. Of course, f may not be constant, particularly near the terminal methyl group of the fatty acid.

From the above discussion, it is clear that the effect of correlated motions is qualitatively similar to the effect of restricting the motion around individual bonds. Thus, for example, it has been shown in section III that the effect of restricted motion is to cause the T_1/T_2 ratio along the chain to decline more slowly than for the free rotation case. Similarly, using the above example, for carbon 10 in a chain undergoing correlated motion with a correlation factor $f = 0.2$, the appropriate T_1 and T_2 values are those calculated for carbon 2 for which the T_1/T_2 ratio will also be large, even if unrestricted internal motion is assumed. It is therefore difficult to separate the effects of motional restriction and motional correlation. One possibility for doing this is based on the demonstration by Batchelor et al.[39] that as the lipid bilayer is heated chemical shifts of the resonances result from the increased populations of gauche configurations along the chain. From this data ΔE, the energy difference between gauche and trans states, and hence σ can be calculated. With experimental values for σ it may be possible to separate the effects of correlated and restricted motion. Estimated values are considered in the following section.

V. Comparison with Experiment

From the calculations presented in the previous sections, it is apparent that gradients in the spin-lattice relaxation rates observed along hydrocarbon chains in which one end is relatively immobilized can be interpreted in terms of three effects: (1) a change in the value of τ_t for each bond; (2) a change in the value of σ for each bond; (3) the cumulative effects of motion about each bond which will lead to a T_1 gradient even if σ and τ_t remain constant along the chain (Figures 3 and 7).

The third effect listed above will be strongly dependent on the degree of correlation of motion as discussed in the previous section. In contrast to the behavior of T_1, the T_2 gradient will depend strongly on effects 2 and 3 listed above but will be nearly independent of the values of τ_t as long as $\tau_0 = 1/6D_0 \gg \tau_t$.

A detailed fit of the data obtained for various lipid systems requires that the internal rotation parameters σ and τ_t be varied for each bond and that provision be made for anisotropic motion of the entire lipid molecule. Such a calculation is beyond the scope of the present paper and given the underdetermined nature of the problem such a fit would not prove entirely enlightening. However, comparison with the available data for several lipid systems does allow some sorting out of the various contributions to T_1 and T_2 mentioned above. The systems considered here are the *n*-hexadecyltrimethylammonium bromide micellar solutions studied previously by Williams et al.[40] and sonicated dimyristoyllecithin vesicles for which the most complete relaxation data is available due to the specifically labeled lecithins studied by Lee et al.[41] Proton decoupled ^{13}C NMR spectra of these systems are given in Figure 9, and the corresponding relaxation data in Table I. Assignments are those of Levine et al.[11] and Barton.[42]

Analysis of the data can be considered in two parts: (1) the coupling of the overall molecular motion to the first resolvable carbon, and (2) the changes in the relaxation parameters along the hydrocarbon chain. The first problem noted above is difficult owing to the possibility of anisotropic motion of the lipid molecules which are likely to be rotating much more rapidly about the long axis parallel to the hydrocarbon chains, anisotropic motion of the rod-shaped micelles, and the difficulty of choosing a completely immobilized atom, C_0. The effects of axially symmetric anisotropic motion on the observed ^{13}C relaxation times have been previously treated by Levine et al.[10]

Table I. ^{13}C Relaxation Parameters for *n*-Hexadecyltrimethylammonium Micelles and Sonicated Dimyristoyllecithin Vesicles in D_2O

Carbon no.	Micelles (42 °C)			Vesicles (52 °C)		
	NT_1, s	$\nu_{1/2}$, Hz	NT_2, s	NT_1,[a] s	$\nu_{1/2}$, Hz	NT_2, s
C-1	0.60	9.8	3.3×10^{-2}			
C-2	0.74	7.5	4.3×10^{-2}	0.40	7.3	4.4×10^{-2}
C-3		6.5	4.9×10^{-2}	0.48	10.6	3.0×10^{-2}
C-7				0.96		
(CH-2)$_n$	0.79			1.04		
C-12				2.76	8.1	3.9×10^{-2}
C-13				3.40	5.2	6.1×10^{-2}
C-14	1.660-12.6	1.2×10^{-1}	11.42	3.3	9.7×10^{-2}	
C-15	2.32	2.9	1.1×10^{-1}			
C-16	8.3	1.6	2.0×10^{-1}			

[a] NT_1 data from ref 41.

and are mathematically equivalent to the effect of combining overall isotropic motion with a single internal rotation for which the axis is chosen parallel to the axially symmetric molecular axis.[26] In making this equivalence, the isotropic diffusion coefficient $D_0 = D_x = D_y$ and the first internal diffusion coefficient is given by $D_i = D_z - D_x$. Allowing for anisotropic molecular motion in aggregated systems may still be insufficient to effectively decouple the local motion from that of the aggregate since *all* of the atoms in the lipid molecule may undergo internal motion in addition to anisotropic motion about the long molecular axis. In order to compensate for the resulting difficulty in defining C_0 for a component of an aggregated complex, it is necessary to postulate several effective internal rotations separating C_0 from the first carbon for which relaxation data can be obtained. Thus, the fatty acid C-2 line width in sonicated dimyristoyllecithin is substantially narrower than the value of several kHz corresponding to a methylene carbon immobilized in a vesicle with a rotational correlation time $\sim 10^{-6}$ s. This difference can only be reproduced quantitatively by assuming that several effective rotations, representing both anisotropic and internal motion, separate C-2 from an atom in the lipid immobilized in the vesicle. Clearly the glycerol methine carbon represents a better, but still not completely satisfactory, choice for C_0 (Figure 9). Since for the systems considered here the T_1 values are dominated by the internal isomerizations and the condition $T_1 \gg T_2$ for most of the resonances, it can be concluded that the D_0 value which appears in the equations is substantially slower than the value corresponding to the T_1 minimum.

The present calculations are, however, better suited to an analysis of the relaxation parameters along the hydrocarbon chain. A feature of the observed T_1 gradient in both the micelles and the sonicated lipid vesicles is an abrupt increase in the NT_1 values for the last two carbons in the chain (Table I). The long T_1 for the terminal methyl carbon in straight-chain hydrocarbons has been interpreted as reflecting an abrupt increase in the diffusion rate about the last bond in the chain.[10] The present calculations suggest that at least part of the effect is due to a change in σ. Thus, for the final methyl rotation the distinction between gauche and trans states vanishes and $\sigma = 1$. Similarly, σ will increase for the penultimate bond since two of the sterically unfavorable g^+g^- and g^-g^+ states corresponding to an internal bond in the chain become essentially g^+t and g^-t states for the $\omega - 1$ bond. Of course, the freer movement about the final bonds can also reflect reduced intermolecular constraints near the end of the chain.

A second feature of the micellar relaxation data is that along the bulk of the chain the T_1 and T_2 gradients are similar. From Figure 5 it is apparent that, neglecting the effect of cross correlations, the T_1/T_2 ratio will remain constant only if σ is extremely small. Alternatively, fitting the data with a larger value of σ requires that there be a considerable degree of correlation in the motion in order to reproduce the small T_1/T_2 gradient. There are several reasons for preferring the latter interpretation. First, if σ is extremely small, the spin-lattice relaxation times become dominated by the slow overall molecular rotation and would probably decrease with increasing temperature. Second, comparison of the spin-lattice relaxation times measured here at 25.2 MHz with those measured at 15.2 MHz[40] indicate relatively small differences. The absence of a frequency dependence is also consistent with a larger value of σ (Figures 3 and 7), although possible differences in sample preparation and solvent (D_2O vs. H_2O) preclude a definite conclusion based on this comparison. Several calculations have been made for a 16-bond chain by noting that for small values of σ, the two time constants appearing in the A matrix (Figure 1) are nearly equal. Setting both time constants equal to τ_s and combining the preexponential factors leads to a considerable reduction in the required calculation time. The quantitative agreement for T_2 using the approximate calculation is excellent even for relatively large values of σ; however, the error in T_1 reaches ~20% for carbon 6 corresponding to $\sigma = 0.3$ (Figures 3 and 4). It should also be noted that the approximation used by Levine et al.[8] for the free rotation model, which is that beyond the first few carbons the orientational autocorrelation function decays as a single exponential, is not valid in the present case. Such calculations suggest that even for σ values as small as 0.05, the T_2 gradient and the T_1/T_2 ratio cannot be reproduced. A more successful attempt to fit the data can be made by using a larger value of σ and a correlation factor as defined in the previous section. For the systems under study, the gauche-trans energy difference is unlikely to be lower than the experimental value of ~1 kcal/mol measured for butane.[43] Using the relation $\sigma = \exp(-\Delta E_g/kT)$, a value of $\sigma = 0.2$ is obtained which is similar to the value deduced for lipid bilayers based on ^2H NMR measurements.[35] Using this value, the observed T_1/T_2 gradient can be reproduced if a correlation factor is introduced. For the micelles, an optimal fit was obtained using the parameters $D_0 = 3.6 \times 10^6\ s^{-1}$ ($\tau_0 = 4.6 \times 10^{-8}$ s), $\sigma = 0.2$, $\tau_t = 1.67 \times 10^{-10}$ s, and a correlation factor, assumed constant along the chain, of 0.25. In obtaining this fit, the relaxation time for the first resolvable carbon has been assumed to be separated by two "effective" internal rotations, representing the anisotropic motion of the lipid and the N-C-1 bond rotation, as discussed above. D_0 then corresponds to the slowest diffusional motion of the micelle. Such a fit clearly represents a considerable approximation; however, as noted above, we are interested primarily in calculating changes in the relaxation parameters along the chain rather than for the (hypothetical) immobilized atom. Fixing the value of σ requires that τ_t be fairly close to the value selected in order to obtain reasonable T_1 values. Calculated NT_1 and NT_2 values for carbons 1, 5, 9, and 13 are given by C-1, 0.578, 0.033; C-5, 0.888, 0.070; C-9, 1.289, 0.182; C-13, 1.667, 0.314. These values agree fairly well with those obtained for the first few resolvable carbons as well as with the C-14 values for the micelles (Table I). Values for carbons not directly calculated can be interpolated. The correlation factor used in this calculations is interpreted to indicate that the cumulative disorder produced by the correlated bond rotations increases at only one-fourth the rate of a calculation assuming the absence of such corre-

lations. Alternatively, extrapolation of the results to carbons 15 and 16 gives a poor result indicating the need to take into account the increase in the value of σ discussed above, a reduction in the degree of correlation for the last few bond rotations, and a decrease in the value of τ_t.

In considering the data obtained for sonicated dimyristoyllecithin vesicles, several distinctive features must first be noted: (1) The fatty acyl C-2 resonance is fairly sharp, as discussed above, indicating that at least several rotations separate it from the hypothetical immobilized atom in the molecule. (2) There is an increase in the ^{13}C line width in going from C-2 to C-3. This feature has been observed in all spectra we have obtained of sonicated dipalmitoyl- and dimyristoyllecithins observed above the liquid crystalline phase transition. It is particularly evident at the highest temperatures where the resonances are most clearly resolved (Figure 10). This observation is not in accord with the theory which has been discussed here which predicts an increase in both the T_1 and T_2 relaxation times in moving away from the most immobilized portion of the molecule, presumed to be the glycerol moiety. This result can be explained if on going from C-2 to C-3, the motion of the appropriate C–H vectors becomes more rapid but less isotropic. It is particularly interesting to note in this regard that the deuterium order parameter obtained for the C-2 carbon at position 2 of the glycerol is smaller than that for the C-3 and the other carbons close to the glycerol.[36,44] (3) The lines appear to be non-Lorentzian possessing broad bases. Non-Lorentzian lines have been predicted for the proton resonances of sonicated vesicles.[5,6] However, there are many other possible explanations for these line shapes. Heterogeneity of vesicle size, the difficulty of completely ^1H decoupling the broad proton resonance, as well as the inequivalence of the resonances corresponding to the two fatty acids esterified to the glycerol C-1 and C-2 carbons may all result in non-Lorentzian line shapes. Such differences are probably particularly important near the beginning of the chain since the deuterons on the two fatty acid C-2 carbons exhibit different order parameters.[44] Differences in the line widths of the glycerol carbons (Figures 9 and 10) also suggest the possibility of different line widths for the two fatty acid carbons. A further source of line width heterogeneity may be differences between the resonances corresponding to the inner and outer leaflets of the bilayer. There is presently substantial evidence for such differences including ESR[45] and ^{13}C NMR spin-lattice relaxation studies[46] indicating greater restriction in the motion of the polar head group of the inner leaflet, ^{19}F chemical shift differences in fluorinated lecithins which have been interpreted to reflect differences in the gauche/trans ratio between the inner and outer layers,[47] and differing preferences of lipids for the inner or outer leaflet as a function of fatty acid unsaturation.[48] Until these effects can be sorted out, it is not possible to consider the observed line widths quantitatively. It is interesting to note that the vesicle relaxation data differ from the micelle data in exhibiting a more pronounced T_1 gradient and a negligible gradient of the apparent line width. Thus, while the fatty acid C-2 line width in both systems is similar, the line width observed for C-12 in the dimyristoyllecithin vesciles or C-14 in the dipalmitoyllecithin vesicles is substantially broader than the C-14 line width in the micelles. Based on the discussion at the beginning of this section, the vesicle data can only be explained by a substantial decrease in τ_t along the chain. Thus, from Figure 5, it is apparent that for constant σ and τ_t along the chain, the T_1/T_2 ratio will decrease moving away from the more immobilized end of the molecule, so that T_2 must increase faster than T_1. This situation can only be overcome by requiring τ_t to decrease along the chain. Therefore, in sonicated dimyristoyllecithin much of the observed T_1 gradient appears to reflect a local increase in the rate of gauche $\rightleftarrows$ trans isomerization rather than increase in the motion of carbons further from the glycerol

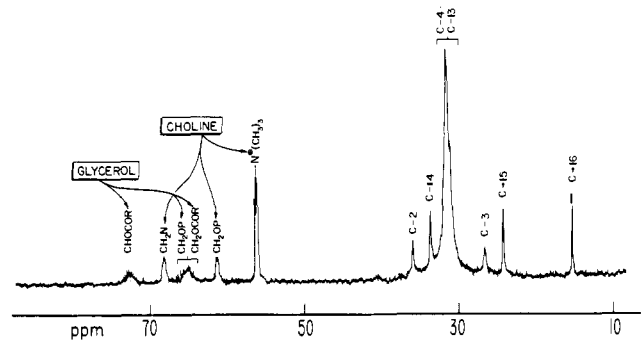

Figure 10. Proton decoupled ^{13}C NMR spectrum of sonicated DL-α-dipalmitoyllecithin vesicles at 85 °C illustrating the line width differences between fatty acyl C-2 and C-3 resonances.

resulting from cumulative bond isomerizations. This conclusion differs from that of Lee et al. based on the analysis of the spin-lattice relaxation data only, using the free internal rotation model, according to which the increase in T_1 represents primarily a cumulative effect with the diffusion coefficients about most of the bonds being equal.[41] The decrease in τ_t suggests instead a gradient in the potential function for the local motions due to differences in intermolecular interactions which are a function of position along the fatty acid chains. Finally, we note that the pattern of increasing T_1/T_2 along the fatty acid chains has similarly been reported in sonicated egg yolk lecithin.[39,49]

It is interesting to consider the above conclusions in light of the existing order parameter data obtained from ^2H NMR studies. Measurements of deuterium order parameters in bilayers indicate a nearly constant value over approximately the first two-thirds of the fatty acid chain and a monotonic decrease over the last third.[36] Recent considerations of the ^2H line widths in vesicles containing ^2H-labeled fatty acids suggest similar order parameters in these systems.[50] Lee et al.[41] have suggested that this ordering may be reflected in the diffusion coefficients calculated from a fit of the ^{13}C spin-lattice relaxation data. Alternatively, according to the present model, this order is reflected in the correlated motions about the carbon-carbon bonds which, as discussed in the previous section, will have the effect of reducing the contribution of cumulative bond rotations on both the T_1 and T_2 values. The observation that the order remains essentially constant along part of the hydrocarbon chain suggests that the observed increase in T_1 is not a cumulative effect but reflects primarily an increase in the local rate of motion about the carbon-carbon bonds which presumably indicates a gradient in the potential for this motion. This is the same conclusion reached above since the order, as reflected in the line width values, changes very slowly implying a very low correlation factor f and/or a low value of σ. The fact that the order parameter is found to decrease over the last third of the hydrocarbon chain suggests that the data should be described by a larger correlation factor f so that the cumulative effects of motion about successive bonds becomes more important. It is also worth noting that at higher temperatures the order parameter in the bilayer does not exhibit a plateau, but decreases monotonically,[51] so that the effects of cumulative motion should be more important in determining the observed T_1 gradient.

Several alternative analyses of the relaxation in various lipid aggregates have utilized two correlation times, a slow value which dominates the line widths and a shorter value which dominates the spin-lattice relaxation.[38,52] Recent computations for ^{13}C nuclei indicate that it is necessary to vary both correlation times along the chain to obtain an accurate fit of the data.[38] Such models can be justified on the assumption that correlated motions such as kink formation become so signifi-

cant that cumulative effects of carbon-carbon bond isomerization on the relaxation times do not have to be considered. As discussed above, this is probably a reasonable assumption for at least the portion of the fatty acyl chain over which the order parameter or ^{13}C line width remains nearly constant. In this portion of the molecule, the T_1 gradient presumably reflects a τ_t gradient as deduced using the model described here. Alternatively, the two correlation time model tends to break down toward the end of the chain. The data can only be fitted by reducing the slow correlation time as well as the correlation time corresponding to internal motion.[38] This result has been interpreted in terms of the probability of uncoupled gauche isomerizations increasing near the end of the chain. The present calculations are completely consistent with such an interpretation. The existence of uncoupled gauche isomerizations requires that the effect of cumulative bond rotations be incorporated into T_1 and T_2 calculations. Thus, the reduction in τ_c obtained using the model of ref 38 becomes an increase in the correlation factor f defined here, implying a decrease in the degree of correlation of the bond isomerizations.

VI. Conclusions

The dominance of ^{13}C relaxation rates by the dipolar interaction with directly bonded protons permits a detailed evaluation of the data for systems undergoing complex motion in terms of various dynamical models. This situation contrasts with that for several other nuclei which have been used to probe various membrane systems, in particular ^{1}H, ^{19}F, and ^{31}P.[1,2,53,54] In these cases, a considerable effort must be made to separate the various possible relaxation mechanisms and, in some cases, the different contributions which can exist for each mechanism. Alternatively, the data analysis for ^{13}C is more similar to that for ^{2}H since, although in the latter case the quadrupolar rather than the dipolar interaction dominates the relaxation, the measured relaxation times are sensitive only to the way in which the particular C-^{2}H vector reorients in space. Thus, the spin-lattice relaxation times obtained for the two nuclei at corresponding positions along the fatty acid chain are proportional.[50]

The multiple internal isomerization model developed here has several important features: (1) As a result of the restriction of the internal motion imposed in the model, relaxation characteristics of the slowly tumbling end of the molecule can extend far into the chain, in contrast to the free internal rotation case. Such characteristics include a reduced NOE, a frequency dependence of the spin-lattice relaxation, and a broad line width as indicated both by the T_2 and T_1/T_2 plots as a function of carbon number. (2) The observed T_1 gradient is considered to reflect in principle three factors: a τ_t gradient, a σ gradient, or a motional gradient reflecting the cumulative effect of each carbon-carbon bond rotation between the most immobilized atom and the carbon whose relaxation is being measured. (3) Gradients in the T_2 values are also predicted to reflect primarily the cumulative motion effect as well as any changes in the value of σ, but to be relatively independent of τ_t. (4) The effects of correlated motions in reducing the contribution of cumulative bond isomerizations to the observed relaxation parameters has been considered semiquantitatively.

These features have several implications for the interpretation of ^{13}C relaxation measurements in systems undergoing complex motions. Perhaps most significant, they indicate that the spin-lattice relaxation times are sensitive to the ordering of the system as well as to the rates of motion about the various carbon-carbon bonds. Thus, although the spin-lattice relaxation behavior can be phenomenologically described by the relation

$$\frac{1}{T_1} = \frac{\gamma_H^2 \gamma_C^2 \hbar^2}{r_{CH}^6} \tau_{eff}$$

the τ_{eff} thus obtained is a function of both the mobility and the ordering of the system. In general, the interpretation of $T_1{}^{13C}$ measured for the Nth carbon in terms of a rate of motion about the Nth bond will be most accurate if the motional correlations are maximal so that the effects of rotations about bonds 1,2, . . . N-1 will be effectively canceled.

In light of the above conclusion, it is particularly interesting to note that the extreme sensitivity of observed line width to various sample preparations is frequently accompanied by a relatively minor sensitivity of the spin-lattice relaxation. Thus, both sonication[39,49,55] and the addition of cholesterol[14] exert a considerably greater effect on the line width than on the spin-lattice relaxation. There has been considerable discussion in the literature concerning whether the observed changes in line width reflect primarily differences in ordering or in the rate of overall molecular tumbling.[3,4,5,31,50] In terms of the above discussion, the T_1 similarities suggest a similarity in the ordering of the lipid system, a result recently deduced on the basis of an analysis of ^{2}H line widths.[50] Thus, a decrease in the internal order of the system, as reflected either by an increased correlation factor (i.e., less correlation of the internal motions), or an increase in the value of σ, should enhance the observed T_1 gradient. It should be noted, however, that there are small differences in the T_1 values measured for sonicated and unsonicated systems which may reflect a difference in the motional correlations. Thus, in the ^{13}C labeled lecithins studied by Gent and Prestegard,[16] the T_1 values for C-2 measured in sonicated and unsonicated preparations are similar while the values for $C_{\omega-2}$ differ by a factor of 1.5, being longer in the sonicated sample. Unfortunately, the problem of separating the effects of τ_t, σ, and f in the two systems prevents an interpretation of the data in terms of order only. Assuming the entire difference to reflect a difference in order, a maximum increase in the correlation factor for the vesicle of ~2 is obtained, where the exact value will be a function of τ_t. Alternatively, it should be noted that studies of specifically ^{13}C labeled sonicated and unsonicated dimyristoyllecithin by Lee et al.[41] reveal smaller differences in the measured T_1 values. To summarize, it is difficult to predict major differences in the ordering of sonicated and unsonicated systems given the similarities in T_1 values and the probability that correlated motions are highly significant in determining the observed T_1 gradient. It should be noted, however, that while vesicle tumbling may be important in determining the observed line widths, internal motions are equally significant, and it is necessary to postulate several effective internal rotations separating the motion of the fatty acyl C-2 carbon from the motion of the lipid vesicle in order to predict a reasonable line width for C-2. This result suggests in turn that motions about the first few bonds from the glycerol may be considerably more disordered than motions along the hydrocarbon chain, perhaps reflecting the lack of highly correlated modes such as kink formation, diffusion, etc.

VII. Materials and Methods

n-Hexadecyltrimethylammonium bromide, L-α-dimyristoyllecithin, and DL-α-dipalmitoyllecithin were purchased from Sigma Chemical Co. and used without further purification. *n*-Hexadecyltrimethylammonium bromide (0.4 M) was dissolved in D_2O and data taken at 41 °C. The lecithins (200 mg/mL) were dissolved in 0.01 M phosphate D_2O (pD 7.2) and sonicated using a Branson W 185 F sonicator for 5-min intervals separated by 5-min cooling intervals until the sample became transparent. Proton decoupled ^{13}C NMR spectra were obtained on a Varian XL-100-15 spectrometer interfaced to a Nova 1210 computer operating in the pulse Fourier transform mode. Samples were locked on the D_2O solvent. A 180°-τ-90°-T pulse sequence was used for the T_1 measurements where T was 8.4 s. T_1 values for the micellar and lecithin vesicle solutions were in excellent agreement with those of ref 40, 41, and 11. The spin-lattice relaxation times given in ref 41 for the sonicated dimyristoyllecithin have been

summarized in Table I due to the more complete data available as a result of studies of specifically ^{13}C labeled lecithins.

Acknowledgment. The authors gratefully acknowledge the assistance of W. E. Wageman in the NMR measurements and the advice and encouragement of Dr. Nicholas A. Matwiyoff during the preparation of this work.

Appendix

The symmetry properties of the A and d matrices may be used to develop an efficient algorithm for evaluating the Fourier transform of $G_N(\tau)$. From Figure 1 it is seen that the A matrix has a twofold symmetry.

$$A_{nn'} = A_{-n',-n} \text{ and } A_{nn'} = A_{n'n} \quad (1A)$$

The reduced Wigner rotation matrix has a similar twofold symmetry (23),

$$d_{nn'}(\beta) = d_{-n'-n}(\beta), \qquad d_{nn'}(\beta) = (-1)^{n-n'}d_{n'n}(\beta) \quad (2A)$$

and it also has the property,

$$d_{nn'}(\beta) = (-1)^{n-n'}d_{nn'}(-\beta) \quad (3A)$$

Equation 3A can be used to rewrite $G_N(\tau)$ in eq 8 as a function of only positive β:

$$G_N(\tau) = \left[\frac{\sigma}{(1+2\sigma)^2}\right]^N \sum_{\substack{abc\ldots n \\ b'c'\ldots n'}} [\exp -(6D_0\tau)] \times [A_{aa}d_{ab}d_{ab'}][(-1)^{b+b'}A_{bb'}d_{bc}d_{b'c}] \times \ldots[(-1)^{m+m'}A_{mm'}d_{mn}(\beta)d_{m'n'}(\beta)] \times [(-1)^{n+n'}A_{nn'}d_{n0}(\beta)d_{n'0}(\beta)] \times \cos[2\pi/3(n-n')] \quad (4A)$$

where only the real part of the imaginary exponential in eq 8 has been retained, because $G_N(\tau)$ is constructed to be a real quantity. If a new four-dimensional array is defined,

$$N_{aa'bb'} \equiv (-1)^{a+a'}A_{aa'}d_{ab}(\beta)d_{a'b'}(\beta)$$

then eq 4A can be written solely in terms of this new array:

$$G_N(\tau) = \left[\frac{\sigma}{(1+2\sigma)^2}\right]^N \sum_{\substack{abc\ldots n \\ b'c'\ldots n'}} [\exp -(6D_0\tau)] \times N_{aabb'}\ldots N_{mm'nn'}N_{nn'00} \times \cos[2\pi/3(n-n')] \quad (5A)$$

With the symmetry relationships (1A) and (2A) the summation in (5A) can be significantly simplified. The N array has the following symmetry properties:

$$N_{aa'00} = (-1)^{a+a'}N_{-a'-a00}, \; N_{aa'00} = N_{a'a00} \quad (6A)$$

These equalities can be used to prove the relationships

$$\sum_{bb'} N_{aa'bb'}N_{bb'00} = \sum_{bb'}(-1)^{a+a'}N_{-a'-abb'}N_{bb'00} = \sum_{bb'} N_{a'abb'}N_{bb'00}$$

$$\sum_{\substack{bb' \\ cc'}} N_{aa'bb'}N_{bb'cc'}N_{cc'00} = \vdots$$

$$\sum_{\substack{bb' \\ cc'}}(-1)^{a+a'}N_{-a'-abb'}N_{bb'cc'}N_{cc'00} = \sum_{\substack{bb' \\ cc'}} N_{a'abb'}N_{bb'cc'}N_{cc'00} \quad (7A)$$

It follows from these relationships that not all the terms in the summation (5A) are unique. Some of the terms cancel each other out and the summation can be shortened. For example, using (6A) and (7A) the first sum in (5A) can be rewritten as

$$\sum_{n=-2}^{+2}\sum_{n'=-2}^{2} N_{mm'nn'}N_{nn'00}\cos\frac{2\pi}{3}(n-n') = \sum_{n=0}^{2}\sum_{n'=-n}^{+n} M_{mm'nn'}M_{nn'00}\cos\frac{2\pi}{3}(n-n') \quad (8A)$$

where

$$M_{mm'nn'} \equiv [N_{mm'nn'} + (1-\delta_{n,-n'})(-1)^{n+n'}N_{mm'-n'-n}] + (1-\delta_{nn'})[N_{mm'n'n} + (1-\delta_{n,-n'})(-1)^{n+n'}N_{mm'-n,-n'}]$$

and δ is the unit matrix. The summation on the left-hand side of eq 8A ranges over 25 terms, while that on the right-hand side ranges over only 9 terms. The M matrix can be used to rewrite the entire summation in (5A)

$$G_N(\tau) = \left[\frac{\sigma}{(1+2\sigma)^2}\right]^N {\sum_{\substack{abc\ldots n \\ b'c'\ldots n'}}}' [\exp -(6D_0\tau)] \times C_aM_{aabb'}\ldots M_{mm'nn'}M_{nn'00}\cos\frac{2\pi}{3}(n-n')$$

where the prime on the summation sign means that the sums run over the restricted range indicated in (8A), the sum over a is from 0 to 2, and the vector C_a has the components $C_2 = 2$, $C_1 = 2$, and $C_0 = 1$.

For a reasonably long model chain the Fourier transform of eq 9A can be evaluated inexpensively with a high-speed computer. It would be prohibitively expensive for all but the shortest of chains to evaluate the original expression for $G_N(\tau)$ in eq 8. We have, however, checked the results for two atoms using eq 8.

References and Notes

(1) A. G. Lee, N. J. M. Birdsall, and J. C. Metcalfe in "Methods in Membrane Biology", Plenum Press, New York, N.Y., 1974.
(2) A. G. Lee, *Prog. Biophys. Mol. Biol.*, **29**, 3–56 (1975).
(3) E. G. Finer, *J. Magn. Reson.*, **13**, 76 (1974).
(4) D. Lichtenberg, N. O. Peterson, J. L. Girardet, M. Kainosho, P. A. Kroon, C. H. A. Seiter, G. W. Feigenson, and S. I. Chan, *Biochim. Biophys. Acta.*, **382**, 10 (1975).
(5) M. Bloom, E. E. Burnell, M. I. Valic, and G. Weeks, *Chem. Phys. Lipids*, **14**, 107 (1975).
(6) H. Wennerstrom and J. Ulmius, *J. Magn. Reson.*, **23**, 431 (1976).
(7) D. Wallach, *J. Chem. Phys.*, **47**, 5258 (1967).
(8) Y. K. Levine, P. Partington, and G. C. K. Roberts, *Mol. Phys.*, **25**, 497 (1973).
(9) Y. K. Levine, P. Partington, G. C. K. Roberts, N. J. M. Birdsall, A. G. Lee, and J. C. Metcalfe, *FEBS Lett.*, **23**, 203 (1972).
(10) Y. K. Levine, N. J. M. Birdsall, A. G. Lee, J. C. Metcalfe, P. Partington, and G. C. K. Roberts, *J. Chem. Phys.*, **60**, 2890 (1974).
(11) Y. K. Levine, N. J. M. Birdsall, A. G. Lee, and J. C. Metcalfe, *Biochemistry*, **11**, 1416 (1972).
(12) J. C. Metcalfe, N. J. M. Birdsall, J. Feeney, A. G. Lee, Y. K. Levine, and P. Partington, *Nature (London)*, **233**, 199 (1971).
(13) P. E. Godici and F. R. Landsberger, *Biochemistry*, **13**, 362 (1974).
(14) P. E. Godici and F. R. Landsberger, *Biochemistry*, **14**, 3927 (1975).
(15) W. Stoffel, B. D. Tunggal, O. Zierenberg, E. Schreiber, and E. Binczek, *Hoppe-Seyler's Z. Physiol. Chem.*, **355**, 1367 (1974).
(16) M. P. Gent and J. H. Prestegard, *Biochem. Biophys. Res. Commun.*, **58**, 549 (1974).
(17) J. D. Robinson, N. J. M. Birdsall, A. G. Lee, and J. C. Metcalfe, *Biochemistry*, **11**, 2903 (1972).
(18) R. E. London, V. H. Kollman and N. A. Matwiyoff, *Biochemistry*, **14**, 5492 (1975).
(19) Y. K. Levine, *J. Magn. Reson.*, **11**, 421 (1973).
(20) P. G. Flory, "Statistical Mechanics of Chain Molecules", Interscience, New York, N.Y., 1969.
(21) J. Seelig, *J. Am. Chem. Soc.*, **93**, 5017 (1971).
(22) J. Seelig, F. Axel, and H. Limacher, *Proc. N.Y. Acad. Sci.*, **222**, 588 (1973).
(23) J. Seelig and W. Niederberger, *Biochemistry*, **13**, 1585 (1974).
(24) W. Hubbel and H. M. McConnell, *J. Am. Chem. Soc.*, **93**, 314 (1971).
(25) M. E. Rose, "Elementary Theory of Angular Momentum", Wiley, New York, N.Y., 1957.
(26) R. E. London and J. Avitabile, *J. Chem. Phys.*, **65**, 2443 (1976).
(27) L. G. Werbelow and D. M. Grant, *J. Chem. Phys.*, **63**, 544 (1975).
(28) L. G. Werbelow and D. M. Grant, *J. Chem. Phys.*, **63**, 4742 (1975).
(29) A. Abragam, "The Principles of Nuclear Magnetism", Clarendon Press, Oxford, 1961.
(30) D. Doddrell, V. Glushko, and A. Allerhand, *J. Chem. Phys.*, **56**, 3683 (1972).
(31) A. F. Horwitz, D. M. Michaelson, and M. P. Klein, *Biochim. Biophys. Acta*, **298**, 1 (1972).
(32) A. F. Horwitz, M. P. Klein, D. M. Michaelson, and S. J. Kohler, *Proc. N.Y. Acad. Sci.*, **222**, 468 (1973).

(33) A. F. Horwitz in "Membrane Molecular Biology", Sinauer Associates, Stamford, Conn., 1972, pp 164-191.
(34) R. Kimmich and A. Peters, *J. Magn. Reson.*, **19**, 144 (1975).
(35) J. Seelig and W. Niederberger, *J. Am. Chem. Soc.*, **96**, 2069 (1974).
(36) A. Seelig and J. Seelig, *Biochemistry*, **13**, 4839 (1974).
(37) H. Schindler and J. Seelig, *Biochemistry*, **14**, 2283 (1975).
(38) M. P. N. Gent and J. H. Prestegard, *J. Magn. Reson.*, **25**, 243 (1977).
(39) J. G. Batchelor, J. H. Prestegard, R. J. Cushley, and S. K. Lipsky, *Biochem. Biophys. Res. Commun.*, **48**, 70 (1972).
(40) E. Williams, B. Sears, A. Allerhand, and E. H. Cordes, *J. Am. Chem. Soc.*, **95**, 4871 (1973).
(41) A. G. Lee, N. J. M. Birdsall, J. C. Metcalfe, G. B. Warren, and G. C. K. Roberts, *Proc. R. Soc. London, Ser. B*, **193**, 253 (1976).
(42) P. G. Barton, *Chem. Phys. Lipids*, **14**, 336 (1975). The one reassignment noted in this reference is actually only a difference in nomenclature (private communication).
(43) A. L. Verma, W. F. Murphy, and H. J. Bernstein, *J. Chem. Phys.*, **60**, 1540 (1974).
(44) A. Seelig and J. Seelig, *Biochim. Biophys. Acta.*, **406**, 15 (1975).
(45) R. D. Kornberg and H. M. McConnell, *Biochemistry*, **10**, 1111 (1971).
(46) B. Sears, W. C. Hutton, and T. E. Thompson, *Biochemistry*, **15**, 1635 (1976).
(47) K. J. Longmuir and F. W. Dahlquist, *Proc. Natl. Acad. Sci. U.S.A.*, **73**, 2716 (1976).
(48) P. L. Yeagle, W. C. Hutton, R. B. Martin, B. Sears, and C. H. Huang, *J. Biol. Chem.*, **251**, 2110 (1976).
(49) B. Sears, *J. Membr. Biol.*, **20**, 59 (1975).
(50) G. W. Stockton, C. F. Polnaszek, A. P. Tulloch, F. Hasau, and I. C. P. Smith, *Biochemistry*, **15**, 954 (1976).
(51) J. H. Davis, K. R. Jeffrey, M. Bloom, M. I. Valic, and T. P. Higgs, *Chem. Phys. Lett.*, **42**, 390 (1976).
(52) C. H. A. Seiter and S. I. Chan, *J. Am. Chem. Soc.*, **95**, 7541 (1973).
(53) M. P. N. Gent, I. M. Armitage, and J. H. Prestegard, *J. Am. Chem. Soc.*, **98**, 3749 (1976).
(54) A. C. McLaughlin, P. R. Cullis, J. A. Berden, and R. E. Richards, *J. Magn. Reson.*, **20**, 146 (1975).

The Effects of Vibrational Averaging on the Calculated Nuclear Spin-Spin Coupling Constants of Ammonia

Paul Solomon and Jerome M. Schulman*

Contribution from the City University of New York, Department of Chemistry, Queens College, Flushing, New York 11367. *Received May 26, 1977*

Abstract: The effects of including molecular vibrations on the calculated nuclear spin-spin coupling constants of a molecule have been studied for the case of ammonia. Both $^1J_{NH}$ and $^2J_{HH}$ were calculated by semiempirical coupled Hartree-Fock perturbation theory as a function of the six internal degrees of freedom and a subsequent vibrational average was computed at two levels of approximation. The first was an averaging over the normal modes, i.e., the small vibrations approximation, while the second procedure treated the inversion motion as a global problem. Rather large vibrational corrections were obtained with $^1J_{NH}$ and $^2J_{HH}$ being reduced ca. 15 and 9%, respectively, from their values calculated at the experimental equilibrium geometry.

I. Introduction

The quantum mechanical calculation of J_{AB}, the isotropic nuclear spin-spin coupling constant between nuclei A and B, remains an active area of theoretical study.[1] Yet most of the calculations of J_{AB} performed assume fixed nuclei at their equilibrium positions, thereby neglecting the role of nuclear motion. When nuclear motion is explicitly considered its treatment is more or less trivial; for example, coupling constants involving methyl protons are reported as statistical averages over a set of conformers. This treatment presumes that the rotamers are to a great degree localized in their respective wells. However, since rotamer interconversion is often quite rapid and the hindered rotational mode is appreciably anharmonic, there could be important contributions to the coupling constant from geometries other than the local minima.

A second example is spin-spin coupling to the nitrogen atom of amines. Here, interconversion between right and left pyramidal forms is rapid, and the inversion mode is anharmonic, so that a consideration of solely one or both quasi-equilibrium structures may be insufficient for a theoretical determination of J. Other situations where nuclear motion may make important corrections to the equilibrium value of J_{AB} are couplings to the proton in a hydrogen bond for which there can be tunneling, and coupling to the central atom of a fluxional molecule.

The correct way to incorporate nuclear motion into a theoretical calculation of the coupling constant within the Born adiabatic approximation[2] is to average J_{AB}, which depends parametrically on a set of nuclear displacements $\mathbf{Q} = (Q_1, Q_2, \ldots)$, over the ground state vibrational wave function. The temperature dependence of J_{AB}, if indeed it is of interest, can be subsequently determined by Boltzmann averaging of the contributions from excited vibrational states.

The only authentic examples of the vibrational averaging of a coupling constant to date appear to have been made for J_{HH} in the hydrogen molecule,[3a-c] J_{HF} in hydrogen fluoride,[4] and for $^2J_{HH}$ in ammonia[5] (over the two totally symmetric degrees of freedom).

Our interest in the possible importance of corrections to spin-spin coupling constants arises from two considerations. Firstly, to the extent to which nuclear motion influences coupling constants in molecules undergoing inversion, hindered rotation, or other fluxional motion, the inferences drawn from the observed coupling constant about the electronic structure at the equilibrium geometry, e.g., hybridizations, may be subject to error. Secondly, since J_{AB} is at present most frequently calculated by INDO finite perturbation theory[6] or some other semiempirical approximate electronic theory,[7] the effects of vibrations could influence the choice of parameters, e.g., spin densities at the nuclei, which are selected to fit experimental data. Important vibrational corrections to J_{AB} for nonrigid molecules might then require that they be treated separately from rigid molecules, or more pessimistically, that J_{AB} might have to be averaged over vibrations before the parameters were chosen.

A possible example of this problem is afforded by the one-bond proton-nitrogen coupling constant in amines, $^1J_{NH}$, where a single product of spin densities, $S_N^2(0)S_H^2(0)$, fails